

Developing Satellite-derived Estimates of Surface Moisture Status

RAMAKRISHNA NEMANI, LARS PIERCE, AND STEVE RUNNING

School of Forestry, University of Montana, Missoula, Montana

SAMUEL GOWARD

Department of Geography, University of Maryland, College Park, Maryland

(Manuscript received 21 October 1991, in final form 17 July 1992)

ABSTRACT

Recent research has shown that the combination of spectral vegetation indices with thermal infrared observations may provide an effective method for parameterizing surface processes at large spatial scales. In this paper, we explore the remotely sensed surface temperature (Ts)/normalized difference vegetation index (NDVI) relationship regarding a) influence of biome type on the slope of Ts/NDVI, b) automating the definition of the relationship so that the surface moisture status can be compared with Ts/NDVI at continental scales. The analysis was carried out using 1) NOAA Advanced Very High Resolution Radiometer (AVHRR) data over a 300-km \times 300-km area in western Montana under various land-use practices (grass, crops, and forests), 2) Earth Resources Observations Systems Data Center continental United States biweekly composite AVHRR data.

A strong negative relationship was observed between NDVI and Ts over all biome types. The similarity of the Ts/NDVI relationships over different biomes indicated that fraction of vegetation cover has strong influence on the spatial variability of Ts. A substantial change in the Ts/NDVI relationship was observed over forests between wet and dry days. In comparison, no change was observed over irrigated crops.

Results from the automated approach agreed well with those using manual selection. At continental scales, the slope of Ts/NDVI is strongly correlated to crop-moisture index values indicating that Ts/NDVI relation is sensitive to surface moisture conditions. Upon further development, this relationship may be useful for parameterizing surface moisture conditions in climate models, decomposition studies, and fire weather monitoring.

1. Introduction

Interactions between the land surface and the atmosphere, and the resulting exchanges of energy and water have a large effect on climate (Shukla and Mintz 1982). The partitioning of energy at the earth's surface, between sensible and latent heat fluxes, is strongly controlled by surface moisture status (Monteith 1981; Shuttleworth 1991). While surface moisture status can be adequately parameterized in energy balance studies for smaller areas, its representation remains a rather difficult task at scales used in most climate models (De Bruin and Holtslag 1982; Avissar and Verstraete 1990). Recent sensitivity analyses of atmospheric circulation models showed strong impacts of surface moisture status on the development of regional as well as global weather patterns (Wilson et al. 1987). Therefore, synoptic and dynamic estimates of surface moisture status would significantly improve climate datasets for proper initialization of global and regional atmospheric models, as well as continental-scale water and energy budget studies (Wetzel and Chang 1988; Wilson et al. 1987).

Recent studies have shown that there is generally a

strong negative relation between remotely sensed spectral vegetation indices, such as the normalized difference vegetation index (NDVI), and surface temperature Ts as measured by thermal infrared emissions (Goward et al. 1985; Goward and Hope 1990; Carlson et al. 1990; Price 1989; Nemani and Running 1989; Smith and Choudhury 1991; Hope et al. 1986). Nemani and Running (1989) found a good relationship ($R^2 = 0.92$) between simulated landscape-level resistance to evapotranspiration and landscape "wetness" as expressed by the slope of the Ts/NDVI relationship. The primary basis for this relationship lies in the unique spectral reflectance-emittance properties of plant leaves in the red and infrared wavelengths, in combination with the low thermal mass of plant leaves relative to soil. Plant spectral reflectance patterns provide a general ability to remotely sense surface variations in green biomass (Tucker 1979). Similarly, the small thermal mass of plant leaves distinguishes their presence from the soil background in thermal infrared observations (Goward et al. 1985). Plant leaves actively exchange absorbed solar radiation through evaporation. During daylight hours, plant leaves maintain a temperature close to air temperature, whereas exposed, dry soil temperatures are much higher than air temperatures because of large thermal mass.

Corresponding author address: Ramakrishna Nemani, University of Montana, School of Forestry, Missoula, MT 59812.

We hypothesize that for dry conditions, as the amount of plant green foliage in a pixel increases, the NDVI will increase as observed T_s emissions decrease, creating a slope in the T_s /NDVI relationship. If the top layer of soil is wetted by rainfall, much of the absorbed solar radiation is consumed in evaporation and the T_s emissions provide no distinction between soils and leaves, creating a flat relationship between the T_s and NDVI. At local scales, however, biotic factors such as vegetation type, and abiotic factors such as topography, net radiation, and clouds, which are not directly related to surface moisture status, can still be expected to influence the T_s /NDVI relationship.

In a previous paper Nemani and Running (1989) explored the temporal variation in the relationship between the T_s /NDVI and surface moisture status for a single biome. In this study, we want to explore the spatial variations between the slope of the T_s /NDVI relationship and surface moisture status across biomes. To accomplish this, we chose to work at the continental scale, where plant distributions are primarily controlled by climate. What affects do plant physiology and life-form have on the T_s /NDVI relationship? How can cloud-contaminated pixels be efficiently excluded from the process of defining the T_s /NDVI relationship? Is the T_s /NDVI related to surface moisture status at continental scales?

2. Methods

a. Effect of biome type on the T_s /NDVI relationship

As an initial study area to test the effects of biome type on the T_s /NDVI relationship, a 300-km \times 300-km area over Montana was chosen. This area is particularly suitable for the present analysis because of the presence of diverse land-use practices, including forestry, agriculture, and grassland (Fig. 1).

Two prominent mountain ranges comprising the northern Rocky Mountains create a barrier to air masses traveling from the Pacific Ocean, leading to a west-to-east precipitation gradient of more than 200 cm yr⁻¹. Conifer forests dominate this mountainous terrain, whereas grasslands and dryland agriculture (wheat) dominate the drier eastside of the Northern Rockies. Agricultural crops (alfalfa and barley) are grown on the windward side of these mountains with the help of irrigation. The temperature defined growing season starts in April and lasts until October. For the natural vegetation, however, growing-season demand for water far exceeds the supply in the summer-dry conditions of western Montana. Therefore, the growing season of natural vegetation is usually cut short by the onset of midsummer drought conditions.

We analyzed NOAA-9 Advanced Very High Resolution Radiometer (AVHRR) image data from its

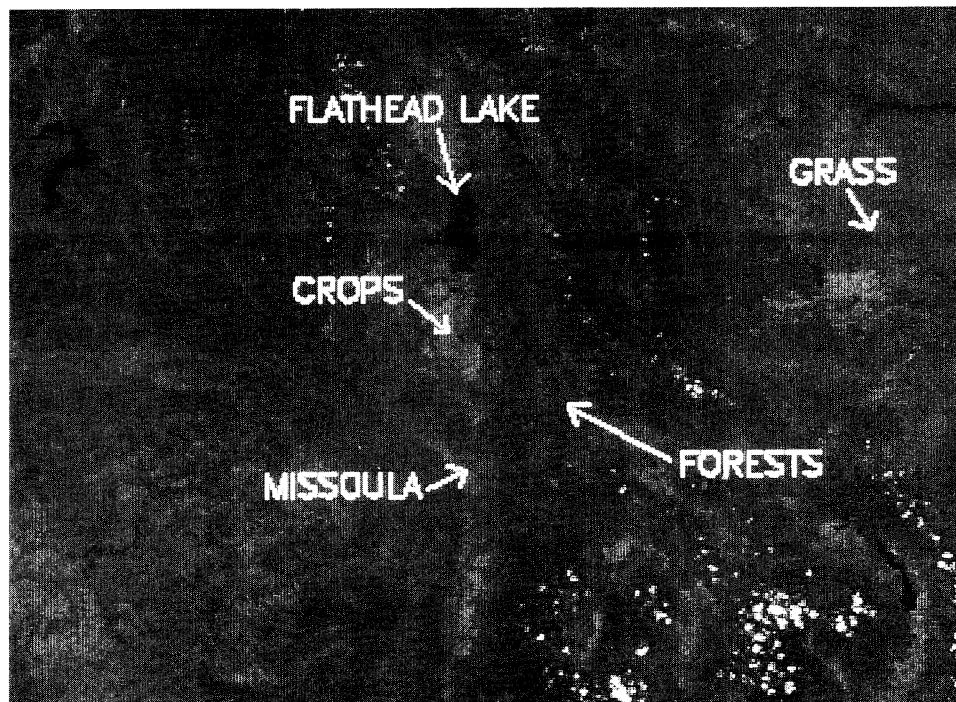


FIG. 1. A gray-level map of the study area in western Montana generated by using near-infrared band of the NOAA AVHRR collected on 14 July 1985. This 380-km \times 280-km area is shown to illustrate the nonhomogeneity in surface conditions that can exist in a single cell of a climate model.

1430-h overpass for three days during the summer of 1985: 3 and 14 July, and 6 August. We normalized for atmospheric differences between the two scenes by comparison of lake radiances. The presence of a large freshwater lake (Flathead Lake) allowed us to subtract the atmospherically scattered radiance in red and near-infrared bands.

Previous research has established significant correlations between IR and red reflectance and canopy properties such as leaf area index, biomass, fraction of vegetation cover (Tucker 1979; Asrar et al. 1984; Peterson et al. 1987; Ormsby 1987; Huette and Jackson 1988). In the present study we utilize the NDVI, a commonly used band combination computed as follows:

$$\text{NDVI} = \frac{\text{NIR} - \text{RED}}{\text{NIR} + \text{RED}}$$

Surface temperature T_s for each pixel was calculated using the split-window technique modified for land surfaces reported by Price (1984), using brightness temperatures derived from thermal channels 4, 5 and by assuming the surface emissivity to be 0.96. This approach is designed to reduce atmospheric water vapor attenuation in the thermal infrared radiance (TIR) region, such that (Price 1984):

$$T_s = T_{b4} + 3.3(T_{b4} - T_{b5}).$$

After the preprocessing steps, two image products, the NDVI and T_s , were generated for each of the two AVHRR images and used for subsequent analysis of the T_s /NDVI relationship.

To observe the influence of different vegetation types on the T_s /NDVI relationship we selected the NDVI and T_s from the 14 July image. With the help of a land-use map of Montana and a classified Landsat/Thematic Mapper (TM) image (acquired on 18 July 1984) covering the study area, we identified three distinct vegetation types: agriculture, grassland, and forest. We extracted the NDVI and T_s values from ten 3-pixel \times 3-pixel grids in each of the three vegetation types (90 pixels each). In addition, 25 pixels from Flathead Lake, 10 pixels with patches of snow from the Mission and Swan mountains, as well as a few cloud-covered pixels were also extracted to display the contrasting T_s /NDVI responses of various surfaces.

b. Automation of defining the T_s /NDVI relationship

To efficiently define the T_s /NDVI relationship across biomes at the continental scale, we needed to automate the process of calculating the slope of the T_s /NDVI. Estimation of the line defining the relationship between NDVI and T_s can be a very difficult and often ambiguous task (Nemani and Running 1989; Goward and Hope 1990). Mixtures of varying surfaces such as clouds and water with vegetation and bare soil

can cause a wide range in temperature for any given NDVI, leading to a T_s /NDVI relationship for which an accurate definition of slope becomes untenable. Previously, the T_s /NDVI relationship was defined by either manual screening of the pixels for cloud-water contamination (Nemani and Running 1989) or using a visual best fit (Goward and Hope 1990). Carlson et al. (1990) used the arch diagram (standard deviation of temperature versus the absolute value of radiometric surface temperature within a pixel subset) to define the asymptotic points of the T_s /NDVI relationship.

We attempted to develop an automated approach in which the algorithm will find the slope of T_s /NDVI through an iterative process, given the NDVI and T_s data from a target area. We utilized a simple sorting algorithm which separates out the upper envelope of pixels forming the T_s /NDVI distribution of the target area and uses these pixels to calculate the slope of the T_s /NDVI relationship.

Briefly, the procedure involves sorting the pixels first based on NDVI and then based on T_s in descending order. Then, a selection process based on the simple rule "if $\text{NDVI}(i+1) < \text{NDVI}(i)$ and $T_s(i+1) > T_s(i)$, then select and save the NDVI and T_s values for the pixel at position i from the double sorted array" is used. A least-squares regression method is used to compute slope and intercept of the relation between NDVI and T_s of the selected pixels. The selection process is then repeated on the previously selected pixels until the difference in R^2 and slope from pass n to pass $n+1$ is less than 10% of those from pass n . The underlying assumption is that pixels forming the upper envelope of the T_s /NDVI distribution are sunlit areas that are in equilibrium with current energy exchange conditions, and will be suitable for defining the representative slope of the T_s /NDVI relationship for the target area.

1) THEORETICAL BASIS

Over land surfaces, temperatures derived from satellite data are a complex function of

- 1) surface properties (canopy cover and density, emissivity, fractions of sunlit and shaded areas in the pixel, moisture status);
- 2) atmospheric conditions (solar radiation, vapor pressure deficit, windspeed, advection); and
- 3) viewing geometry of the sensor.

In mountainous terrain, topography also plays a predominant role in influencing T_s through changes in solar radiation loading (south-facing versus north-facing slopes), and adiabatic lapse rates.

Given similar conditions of atmosphere, soil water, surface emissivity, and viewing geometry, surface temperature varies with canopy cover and density due to latent heat transfer or changes in thermal inertia (Carl-

son et al. 1990; Choudhury 1991; Goward et al. 1985). Factors such as cloud contamination and differences in the fraction of shaded area contribute, however, to *y*-axis variation in *T_s* at any given NDVI. For example, a tail is often visible in many *T_s*/NDVI scatterplots resulting from cloud contamination which reduces both the NDVI and surface temperature. Therefore, uncontaminated pixels should be located in the upper portions of the *T_s*/NDVI distribution.

Differences in fractions of sunlit and shaded areas in the AVHRR pixel would also contribute to the variation along the *y* axis in *T_s* at a given NDVI. As the fraction of sunlit area of the surface as viewed by the sensor increases, so does the *T_s* and NDVI as recorded by the sensor. Therefore, these sunlit pixels which have the highest temperature for a given NDVI will define the upper bound of the *T_s*/NDVI relationship.

Fraction of canopy cover has similar influence on surface temperature. As the viewing angle deviates from nadir, fraction of bare surface viewed by the sensor decreases resulting in lower surface temperatures. Therefore pixels at the top of the distribution should consist of those viewed from nadir or near-nadir view angles.

2) EFFECT OF WINDOW WIDTH FOR DEFINING *T_s*/NDVI RELATIONSHIP

A suitable range of NDVI must be present in the target area so as to compute the *T_s*/NDVI relation. The target area can be assumed to consist of a mixture of vegetation, bare soil, dead vegetation, or forest litter. At the scale of an AVHRR pixel, the properties of individual components cannot be resolved; however, the suitability of the window size in producing a range of NDVI can be explored from the data itself. The NDVI of a mixed pixel can be written as

$$NDVI_p = (f)NDVI_v + (1 - f)NDVI_n,$$

where *v* and *n* denote vegetation and nonvegetation (Price 1989). Since a dense, uniform vegetation cover does not provide us with a range of NDVIs, the surface inhomogeneity plays a key role in the definition of a target size for defining the *T_s*/NDVI relationship. We are interested in the scale at which surface heterogeneity is sufficient to define a stable *T_s*/NDVI relation. We explored this question by analyzing the scatterplots of *T_s*/NDVI for various window sizes: 50 km × 50 km, 30 km × 30 km, and 10 pixel × 10 pixel for crops, grasslands, and forests for both 14 July and 6 August datasets.

c. Relationship between the *T_s*/NDVI and moisture status

1) REGIONAL

The effect of changes in surface moisture status on *T_s*/NDVI relationship was studied over the three

landcover types (crops, grasses, and forests) using AVHRR data collected on 14 July and 6 August. Surface conditions were very dry on 14 July, with no precipitation during the previous four weeks. In contrast, 6 August was relatively wet with 5 cm of precipitation received during the previous week. Average daily climate conditions for the two days recorded in selected locations around the scene are given in Table 1.

2) CONTINENTAL

At continental scales, our primary objective was to gain a sample of surface temperatures and NDVIs large enough to adequately define the slope of the *T_s*/NDVI relationship within and across different biomes. Also, continental-scale datasets, such as the crop-moisture index (CMI) [National Weather Service (NWS) 1977] provide a means to qualitatively evaluate the usefulness of the *T_s*/NDVI for estimating surface moisture status. To effectively address this scale of question, yet avoid the image processing required for large datasets, we utilized the Earth Resources Observations Systems (EROS) Data Center (EDC) 1990 biweekly composites of National Oceanic and Atmospheric Administration (NOAA) AVHRR 1-km data to calculate our *T_s*/NDVI relationship. These data are preprocessed and registered at EDC, and consist of one year of biweekly composites for the continental United States contained on five compact disks (Loveland et al. 1991).

We chose two different biweekly composites: 25 May–7 June representing late spring conditions, and 6 July–19 July representing midsummer conditions for the continental United States. For each of these composites, NDVI and *T_s* were calculated as previously described.

Twenty climatic zones were chosen at random to study the relation between the slope of *T_s*/NDVI and CMI. For each climatic zone, the average slope of *T_s*/NDVI was computed using a 40-pixel × 40-pixel window for each of the composite periods. The average slopes were related to CMI data for each climatic zone obtained from the *Weekly Weather and Crop Bulletin* (NOAA/NWS/United States Department of Agriculture).

TABLE 1. Meteorological conditions recorded (1400 h) at weather stations situated in various biomes: grasses (Great Falls), crops (Polson), and forests (Lubrecht Experiment Forest headquarters) on 14 July and 6 August.

	Polson		Great Falls		LEF, HQ	
	14 July	6 Aug	14 July	6 Aug	14 July	6 Aug
<i>T_{air}</i> °C	26.00	25.00	25.00	25.00	28.0	26.0
Vapor pressure deficit (mb)	22.00	21.00	21.00	22.00	24.0	21.0
Radiation (W m ⁻²)					850.0	730.0

It is important to note that in this preliminary analysis, we did not attempt to standardize the T_s /NDVI relations for local meteorological conditions such as wind speed, air temperature, and humidity. The compositing procedures used to produce this biweekly AVHRR dataset further complicate any attempts for standardizing for local meteorological conditions. Consequently results from this analysis should be viewed with caution.

3) CROP-MOISTURE INDEX

The commonly reported moisture availability indices on a continental scale are (a) Palmer drought-severity index (PDSI) and (b) crop-moisture index (National Weather Service 1977). Both indices are calculated based on estimates of potential evapotranspiration and soil moisture depletion. In the present

analysis, we chose the CMI over PDSI because CMI (reported weekly) depicts changes in soil moisture situation more rapidly than does the PDSI. Therefore, CMI values may indicate more favorable moisture conditions over a particularly wet or dry month even in the middle of a serious long-term wet or dry period.

3. Results and discussion

a. Effect of Biome type on T_s /NDVI relationship

The NDVI of forest, grasses, and crops varied between 0.1 and 0.65 and T_s ranged from 32° to 52°C. NDVI ranged from -0.1 to 0.03 for water, clouds, and snow surfaces. Water temperature in Flathead Lake was estimated to be 20°C. While cloud-covered pixels had the lowest temperature (5°C), the temperature of pixels with variable snow cover ranged between 6° and 18°C. It appears from Fig. 2 that pixels contaminated

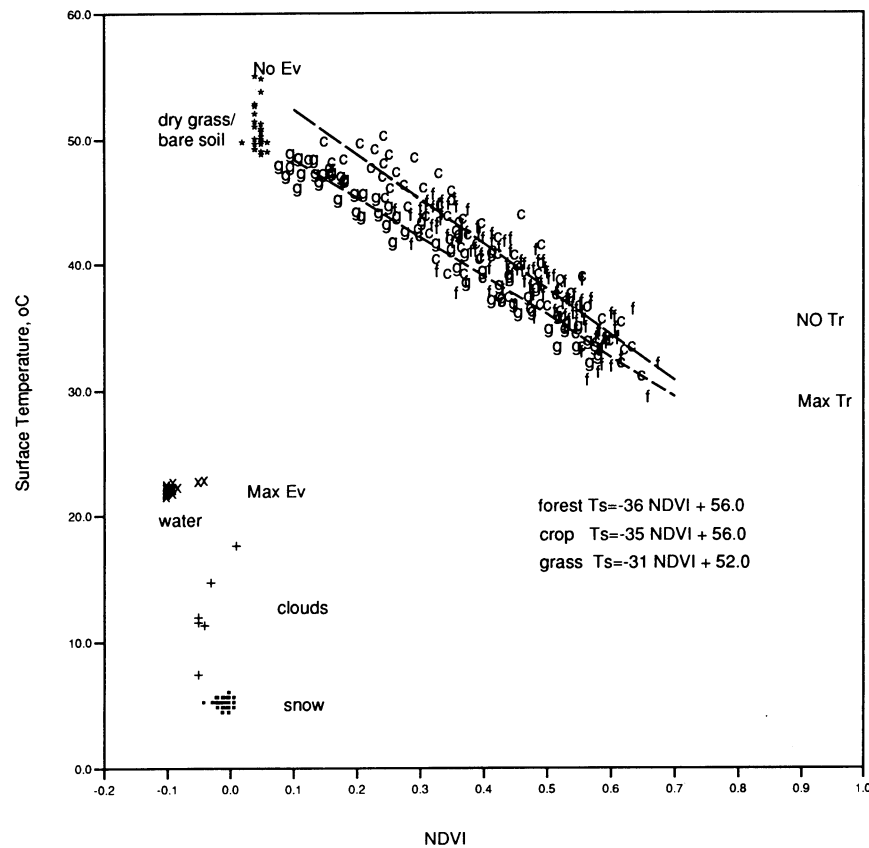


FIG. 2. Observed relations between NDVI and T_s in crops (c), grasses (g), and forests (f) in a 380-km \times 280-km area in western Montana on 14 July 1985. Temperature from freely evaporating water surface over Flathead Lake indicates potential evaporation conditions (Max Ev). On the other hand, surface temperatures over dry grass and bare soil represent conditions of no evaporation (No Ev). The variation in temperatures between Max Ev and No Ev at low NDVI values occurs mainly due to differences in surface moisture availability. The other two limits at high NDVI values represent surface temperature responses to maximum transpiration (Max Tr) and no transpiration (No Tr). Inherent differences in canopy resistance properties would be responsible for variation between No Tr and Max Tr. It is evident from this study that fraction of canopy cover is an important factor in controlling surface temperatures.

with clouds, water, and moisture drawn in from vegetation that they can be easily eliminated. As the amount of "contamination" within a pixel decreases, however, they can become more difficult to automatically eliminate.

The presence of such heterogeneity in surface Ts and temperatures, resulting in a range of evaporation rates, is common even at the scale of mesoscale atmospheric circulation models. From Fig. 2 we can conceptualize four domains in the relationship between NDVI and surface temperature. The location of these domains in Fig. 2 is controlled by the various rates of evaporation and transpiration operating in the study area. At low NDVI values (less than 0.1, generally associated with the absence of vegetation), the low Ts of Flathead Lake results from high rates of evaporation (Max Ev domain), whereas the high Ts of areas of dry grass and/or bare soil results from little or no evaporation (No Ev domain). At low NDVIs, a change in surface temperature between the Max Ev and No Ev domains would be directly controlled by available moisture at the soil surface (Shuttleworth 1991). At the highest NDVI values (greater than 0.4, associated with complete vegetation cover) a change in surface temperature is associated with a change in vegetation transpiration Tr. Movement between the Max Tr and No Tr domains of Fig. 2 would occur in response to changes in canopy resistance to transpiration (Shuttleworth 1991; Smith and Choudhury 1991). It must be noted that the NDVI value at which a complete canopy cover is assured can vary depending upon vegetation types (Price 1989).

NDVIs varied between 0.28 and 0.65 for forests, 0.1 and 0.64 for crops, and 0.05 and 0.55 for grasses, while Ts varied between 35° and 52°C for forests, 32° and 50°C for crops, and 33° and 50°C for grasses. A strong relation was observed between NDVI and Ts over all the vegetation types: forests [$T_s = -36(\text{NDVI}) + 56$, $R^2 = 0.92$], crops [$T_s = -35(\text{NDVI}) + 56.0$, $R^2 = 0.93$], and grasses [$T_s = -31(\text{NDVI}) + 52.0$, $R^2 = 0.89$]. Though the Ts/NDVI of grasslands has slightly lower slope and intercept values, in the absence of information about wind conditions we cannot conclude whether the lower surface temperatures are due to higher evapotranspiration rates or higher turbulent mixing.

At small scales, surface temperatures of plant canopies or soils can exhibit a high degree of spatial variability (Choudhury 1991) due to spatial variations in root-zone soil water, differential soil drying rates, and vegetation physiology. But at the larger scale of an AVHRR pixel (1.1 km) such variability cannot be resolved. Therefore, variation in surface temperature at the AVHRR scale appears to be due primarily to fractional vegetation cover, while vegetation physiology and physiognomy are of secondary importance. Because NDVI is related to fractional vegetation cover (Huette and Jackson 1988; Ormsby et al. 1987;

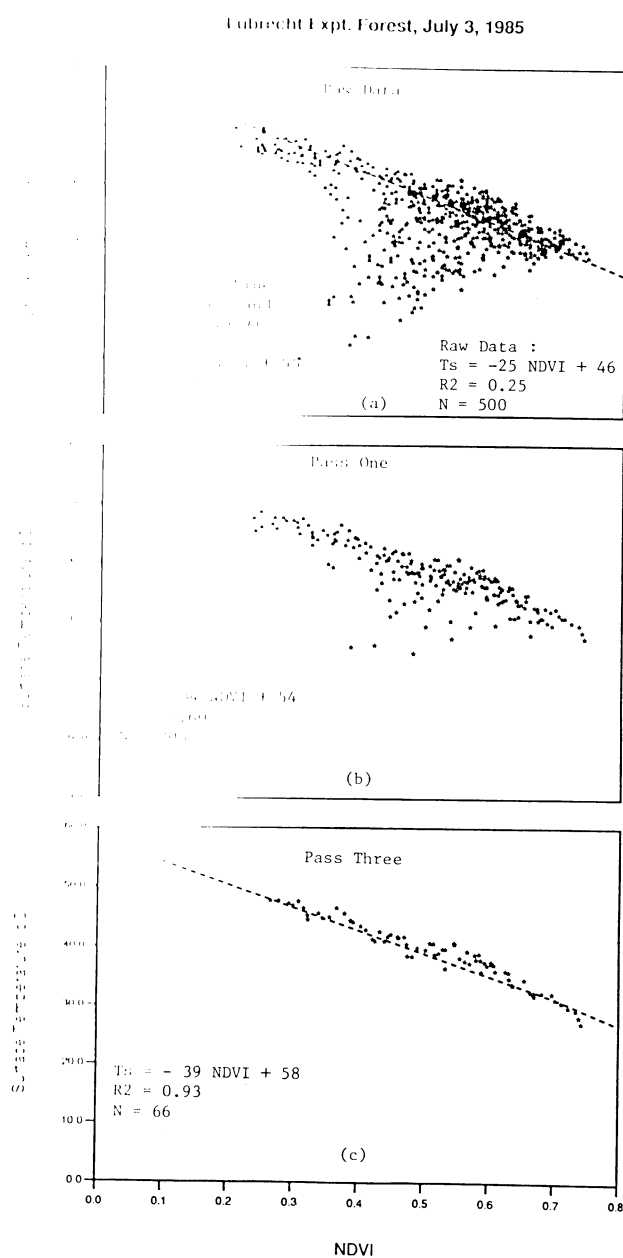


FIG. 3. Illustration of the results from the algorithm developed to automatically define the relation between NDVI and Ts. (a) Observed relation between NDVI and Ts from the raw data over a 20-km \times 25-km area on a partly cloudy 3 July 1985. (b) and (c) The relations defined by the algorithm at the end of pass 1 and pass 3, respectively. A stable relation was obtained at the end of pass 3. The regression line shown in (a) was fit by manually removing cloud-contaminated pixels (Nemani and Running 1989). (See Table 2.)

Choudhury 1991) and Ts is strongly controlled by fractional vegetation cover (Hatfield et al. 1982; Sader 1986), the slope of the Ts/NDVI relationship should be primarily controlled by fractional vegetation cover, surface moisture status, and local meteorological conditions.

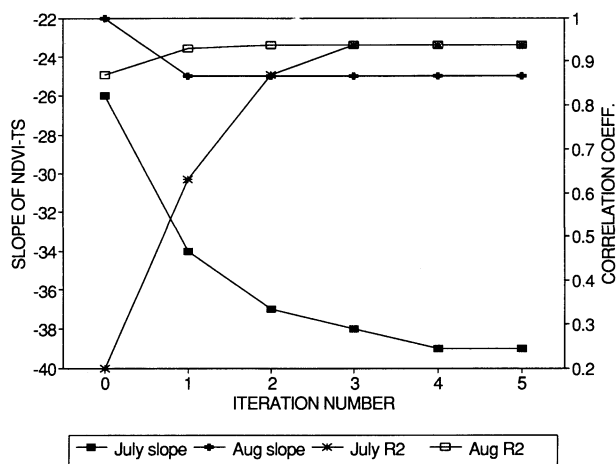


FIG. 4. Changes in the relation found (slope and R2) during the iterative process when the algorithm is applied on a 20-km \times 25-km area (Nemani and Running 1989) on a partly cloudy 3 July compared to a sunny 6 August. While it took three iterations on 3 July, only one iteration was needed on 6 August to develop a stable relation between NDVI and Ts.

b. Automation of defining the Ts/NDVI relationship

Figure 3a shows the observed relation between NDVI and Ts for the 20-pixel \times 25-pixel area on 3 July at Lubrecht Experimental Forest [$T_s = -25(\text{NDVI}) + 46$, $R^2 = 0.25$]. The cloud-contaminated pixels, visible as a tail in the distribution, contributed to the poor relationship. Scatterplots of the selected pixels at the end of pass 1 and 3 from the automation algorithm are shown in Figs. 3b and 3c. During the first pass much of the cloud contamination was eliminated as the slope changed from -25 to -34 and R^2 from 0.2 to 0.6. Results of relation from subsequent passes are shown in Fig. 4. At the end of pass 3 a stable relationship was obtained (Fig. 4) and the scatterplot after pass 3 [Fig. 3c, $T_s = -39(\text{NDVI}) + 58$] shows that there can be no further improvement.

While it took 3 passes to define a stable relationship on a partly cloudy day (3 July), only one pass was required on a clear day, 6 August (Fig. 4). The results at the end of the default pass 1 barely met the criterion of 10% change in slope and R^2 . The strong relation between NDVI and Ts on 6 August can be attributed

to: a) a lack of cloud contamination, and b) the y -axis variation in T_s at a given NDVI due to differences in the fraction of sunlit and shaded areas is small under wet surface conditions.

To compare the relationships determined by the automated approach with our previously reported results for the Lubrecht Experimental Forest, we ran the algorithm on the 20-km \times 25-km area used previously (Nemani and Running 1989). Table 2 shows the T_s /NDVI relationships computed from the manual best-fit approach (Nemani and Running 1989) and the automated approach developed in this study for all the eight days during the summer of 1985. There is a good agreement between the two approaches, though the values of intercept are slightly higher from the automated approach. Such discrepancies in intercept are expected because the regression line in the case of our automated method passes through the envelope of pixels rather than the middle of the distribution. The consistent performance of the automated approach over the eight days indicates, however, that the process of defining T_s /NDVI relation can be automated over a large target area.

c. Effect of window width for defining Ts/NDVI relationship.

Date of imagery (and consequently moisture status) had no effect on optimal window size within any given vegetation type; however, optimal window size changes with vegetation type. For crops, variations in window width from 10 to 50 pixels lead to a change in slope of only 8%, suggesting that a window size of 10 \times 10 pixels is adequate for defining the T_s /NDVI relationship in crops. The variation in crop NDVI is probably controlled by fractional vegetation cover as it relates to varying crop phenology. For grasslands, a reliable definition of the slope could not be determined at either the 10- or 30-pixel widths. Only at 50 \times 50 pixels did the inclusion of irrigated pastures allow us to determine the slope with confidence.

In forests, most of the spatial variation in NDVI was captured using 30-pixel \times 30-pixel windows. The range of forest T_s and NDVI is most likely controlled by topographic variations which cause variations in mi-

TABLE 2. Comparison of the relationships obtained over forests at LEF by manual screening of pixels (Nemani and Running 1989) and by automated algorithm for eight days during the summer of 1985.

Date	Manual screening	R^2	Automated screening	R^2
16 May	$T_s = -34(\text{NDVI}) + 47$	0.73	$T_s = -33(\text{NDVI}) + 50$	0.97
22 June	$T_s = -37(\text{NDVI}) + 53$	0.78	$T_s = -38(\text{NDVI}) + 55$	0.95
3 July	$T_s = -45(\text{NDVI}) + 60$	0.78	$T_s = -39(\text{NDVI}) + 58$	0.95
14 July	$T_s = -44(\text{NDVI}) + 55$	0.91	$T_s = -41(\text{NDVI}) + 63$	0.95
6 August	$T_s = -28(\text{NDVI}) + 42$	0.88	$T_s = -23(\text{NDVI}) + 42$	0.93
17 August	$T_s = -32(\text{NDVI}) + 41$	0.85	$T_s = -31(\text{NDVI}) + 42$	0.97
29 August	$T_s = -34(\text{NDVI}) + 53$	0.77	$T_s = -36(\text{NDVI}) + 57$	0.97
25 September	$T_s = -24(\text{NDVI}) + 28$	0.74	$T_s = -23(\text{NDVI}) + 30$	0.89

TABLE 3. Observed Ts/NDVI relationships over different vegetation types on dry (14 July) and wet (6 August) days.

Date	Crops	Grasses	Forests
14 July	$-39(\text{NDVI}) + 60$	$-32(\text{NDVI}) + 53$	$-35(\text{NDVI}) + 55$
6 August	$-39(\text{NDVI}) + 54$	$-32(\text{NDVI}) + 45$	$-18(\text{NDVI}) + 41$

croclimate and leaf area display. Since the range of NDVIs captured at 30×30 and 50×50 pixels is almost equal, we tested if placing the 30×30 window at various locations inside the 50×50 would have any effect on the computed slope. The slopes determined from these variously placed grids varied from -33 to -39 . The variation in the slope of the Ts/NDVI relationship, as well as overall target area moisture status, is controlled by the amount and distribution of north- and south-facing slopes within a particular 30×30 window.

Since forested areas are associated with mountainous terrain in the northwest United States, topography poses a problem for determining the slope of Ts/NDVI relation. The influence of topography is especially crucial in areas where elevational gradients of temperature and precipitation occur over short horizontal distances to produce contrasting vegetation types. Figure 5 shows such a scenario where increasing window size produced two distinct relationships. Pixels in relation 1 are located at lower elevations and they represent various mixtures of grass and trees. On the other hand, pixels shown in relation 2 are located on a plateau which is 700 m higher in elevation. As the window size increased more pixels from high-elevation areas are included resulting in lower slope and intercept values. The lower surface temperatures at high elevations are a function of (a) lower air temperatures due to adiabatic cooling, and (b) higher amounts of surface moisture due to orographically generated precipitation. Consequently, while relating the changes in the Ts/NDVI relation to surface processes it is important to keep the topography invariant or explicitly account for its effects on NDVI and surface temperature brought about by changes in atmospheric conditions.

d. Relationship between Ts/NDVI and moisture status

1) REGIONAL

The largest change in slope between dry and wet days was observed in open forests, and there was little change in slope for crops or grasslands (Table 3). Over grassland and crops, the slope between 14 July and 6 August remained unchanged. No change in slope would be expected over irrigated crops because moisture status remains relatively constant due to regular irrigation. In grasslands, the 50-pixel \times 50-pixel target area is too small for defining a suitable range in NDVI to calculate a Ts/NDVI relationship. Only when the 50-pixel \times 50-pixel grassland grid included irrigated

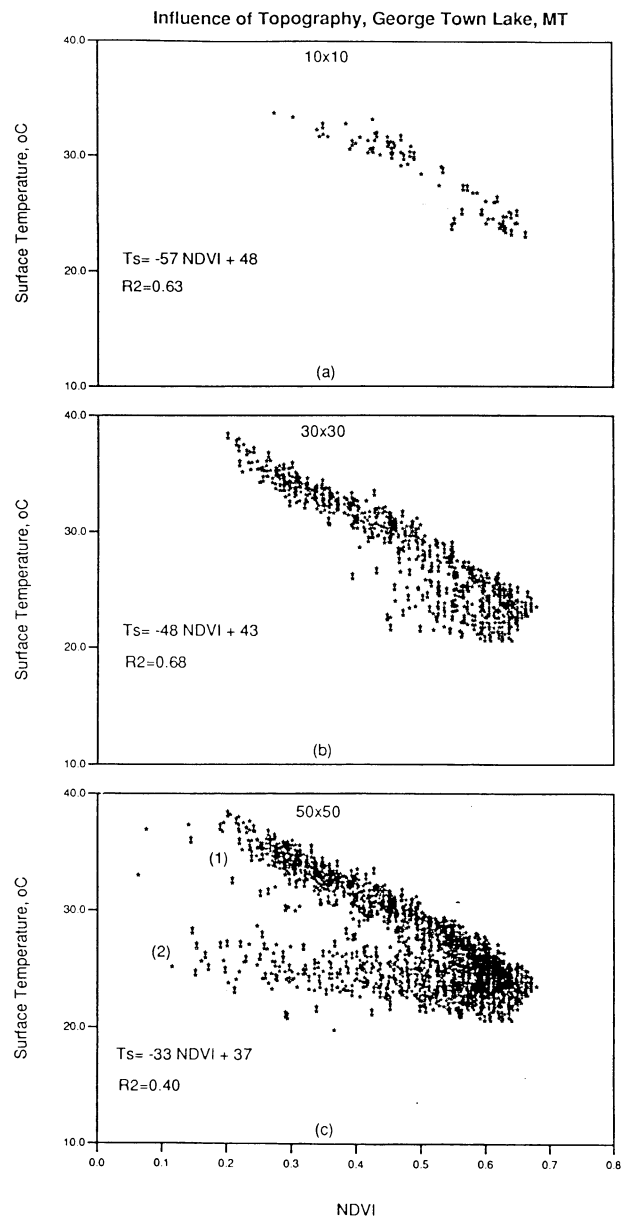


FIG. 5. Influence of topography on Ts/NDVI relation observed over an area near Georgetown Lake, western Montana at grid sizes: (a) 10 km, (b) 30 km, and (c) 50 km. As the grid size increased, more pixels from higher elevations were included leading to a reduction in both slope and intercept of the relation. At 50 km \times 50 km, two relations emerged, 1) grass-tree mixtures at low elevation, and 2) alpine vegetation at higher elevations.

the Ts/NDVI relationship. The moisture status of irrigated pasture would remain constant between the two dates, so little change in the slope would be expected for our 50 \times 50 grassland grid. In natural vegetation that exhibits morphological changes in response to environmental stress (such as grasses or crops), the NDVI alone can provide information about surface resistance (Sellers 1985).

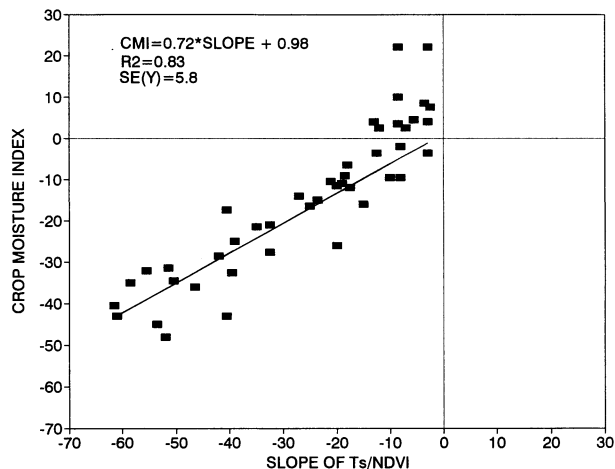


FIG. 6. Relation between the slope of Ts/NDVI and crop-moisture index for 20 climatic zones observed over two biweekly periods (25 May–7 June and 6 July–19 July 1990).

2) CONTINENTAL

A strong correlation ($R^2 = 0.83$) was found between crop-moisture index and the slope of Ts/NDVI for the selected climatic zones (Fig. 6). For climatic zones with CMI greater than zero (wet), the slope values ranged between 0 and 12. These values were not included in the relation, as the Ts/NDVI relationship is related to degree of dryness not wetness. As the CMI became increasingly negative, the slope values responded similarly.

In spite of the strong correlation, there is considerable scatter (standard error of 5.8) in the relation. We believe several factors contribute to the observed variation:

- CMI is based on precipitation data collected at a few stations in the climatic zone,
- during a biweekly composite period the CMI conditions can change drastically, and
- changes in atmospheric conditions could have strong impact on observed NDVI and Ts values.

4. Conclusions

The combination of spectral vegetation indices with thermal infrared measurements from NOAA AVHRR appears to be a useful tool for studying land-atmosphere interactions. At coarse resolutions, the fraction of canopy cover seems to play an important role in regulating surface temperatures observed from satellite sensors.

A substantial change in the slope of Ts/NDVI relation between wet and dry days was observed over forests for a 50-pixel \times 50-pixel target area; however, vegetation type and topography are important in determining the size of the target-area grid size. Grasslands, because of their general lack of topographic

variability relative to forests, require a larger grid size to adequately define a slope of the Ts/NDVI relationship. No change was observed in the Ts/NDVI relation over irrigated crops, indicating that under optimum conditions of temperature and water the NDVI alone is suitable for estimating minimum canopy resistance.

On a continental scale, the slope of Ts/NDVI is correlated to moisture availability conditions. The possibility of inferring surface moisture conditions from satellite data on a global scale would be significant for climate modeling, global decomposition estimates, and fire weather monitoring.

Acknowledgments. Funding has been provided primarily from NSF, Grant BSR-8817965, and NASA, Grants NAGW-252, NAS5-30920. We would like to thank Dr. John Price for his valuable comments.

REFERENCES

- Asrar, G., M. Fuchs, E. T. Kanemasu, and J. L. Hatfield, 1984: Estimating absorbed photosynthetically active radiation and leaf area index from spectral reflectance in wheat. *Agron. J.*, **76**, 300–306.
- Avissar, R., and M. M. Verstraete, 1990: The representation of continental surface processes in atmospheric models. *Rev. Geophys.*, **28**, 35–52.
- Carlson, T. N., E. M. Perry, and T. J. Schmugge, 1990: Remote estimation of soil moisture availability and fractional vegetation cover over patchy vegetation. *Agric. and Forest Meteorol.*, **52**, 44–60.
- Choudhury, B. J., 1991: Multispectral satellite data in the context of land surface heat balance. *Rev. Geophys.*, **29**, 217–236.
- De Bruin, H. A. R., and A. A. M. Holtslag, 1982: A simple parameterization of the surface fluxes of sensible and latent heat during daytime compared with the Penmon–Monteith concept. *J. Appl. Meteorol.*, **21**, 1610–1621.
- Goward, S. N., and A. S. Hope, 1990: Evapotranspiration from combined reflected solar and emitted terrestrial radiation: Preliminary FIFE results from AVHRR data. *Adv. Space Res.*, **9**, 239–249.
- , G. D. Cruickshanks, and A. S. Hope, 1985: Observed relation between thermal emission and reflected spectral radiance of a complex vegetated landscape. *Remote Sens. Environ.*, **18**, 137–146.
- Hatfield, J. L., J. P. Millard, and R. C. Gottelman, 1982: Variability of surface temperature in agricultural fields of central California. *Photo. Eng. Remote Sens.*, **48**, 1319–1325.
- Hope, A. S., D. E. Petzold, S. N. Goward, and R. M. Ragan, 1986: Simulated relationships between spectral reflectance, thermal emissions and evapotranspiration of a soybean canopy. *Water Res. Bull.*, **22**, 1011–1019.
- Huette, A. R., and R. D. Jackson, 1988: Soil and atmosphere influences on spectra of partial canopies. *Remote Sens. Environ.*, **25**, 89–105.
- Loveland, T. R., J. W. Merchant, D. O. Ohlen, and J. F. Brown, 1991: Development of land-cover characteristics database for the conterminous U.S. *Photo. Eng. Remote Sens.*, **57**, 1453–1463.
- Monteith, J. L., 1981: Evaporation and surface temperature. *Quart. J. Roy. Meteor. Soc.*, **107**, 1–27.
- National Weather Service, 1977: Crop moisture index. *Tech. Procedures Bull.*, **204**, Met. Services Div., Silver Spring, MD.
- Nemani, R. R., and S. W. Running, 1989: Estimation of surface resistance to evapotranspiration from NDVI and thermal-IR AVHRR data. *J. Appl. Meteorol.*, **28**, 276–284.

- Ormsby, J. P., B. J. Choudary, and M. Owe, 1987: Vegetation spatial variability and its effect on vegetation indices. *Int. J. Remote Sens.*, **8**, 1301–1306.
- Peterson, D. L., M. A. Spanner, S. W. Running, and K. B. Teuber, 1987: Relationship of thematic mapper simulator data to leaf area index of temperate conifer forests. *Remote Sens. Environ.*, **22**, 323–341.
- Price, J. C., 1984: Land surface temperature measurements from the split window channels of NOAA-7/AVHRR. *J. Geophys. Res.*, **100**, 81–92.
- , 1989: Using the spatial context in satellite data to infer regional scale evapotranspiration. *IEEE Trans. Geosci. Remote Sens.*, **28**, 940–948.
- Sader, S. A., 1986: Analysis of effective radiant temperatures in a Pacific Northwest forest using thermal infrared multispectral scanner data. *Remote Sens. Environ.*, **19**, 105–115.
- Sellers, P. J., 1985: Canopy reflectance, photosynthesis and transpiration. *Int. J. Remote Sens.*, **6**, 1335–1372.
- Shukla, J., and Y. Mintz, 1982: Influence of land-surface evapotranspiration on the earth's climate. *Science*, **215**, 1498–1501.
- Shuttleworth, W. J., 1991: Insight from large-scale observational studies of land/atmosphere interactions. *Land Surface-Atmosphere Interactions for Climate Modeling, Observations, Models and Analysis*, E. F. Wood, Ed., Kulwer Academic, 300–320.
- Smith, R. C. G., and B. J. Choudhury, 1991: Analysis of normalized difference and surface temperature observations over southeastern Australia. *Int. J. Remote Sens.*, **12**, 2021–2044.
- Tucker, C. J., 1979: Red and photographic infrared linear combinations for monitoring vegetation. *Remote Sens. Environ.*, **8**, 127–150.
- Wetzel, P. J., and J. T. Chang, 1988: Evapotranspiration from non-uniform surfaces: A first approach for short-term numerical weather prediction. *Mon. Wea. Rev.*, **116**, 600–621.
- Wilson, M. F., A. Henderson-Sellers, R. E. Dickinson, and P. J. Kennedy, 1987: Sensitivity of the Biosphere-Atmosphere Transfer Scheme (BATS) to inclusion of variable soil characteristics. *J. Climate Appl. Meteor.*, **60**, 341–362.